ELSEVIER

Bioelectrochemistry and Bioenergetics 47 (1998) 151–161

BIOELECTROCHEMISTRY AND BIOENERGETICS

Local transport regions (LTRs) in human stratum corneum due to long and short 'high voltage' pulses

Uwe F. Pliquett [a,*], Rita Vanbever [b], Veronique Preat [b], James C. Weaver [c]

[a] *Faculty of Chemistry, PCIII, University of Bielefeld, D-33615 Bielefeld, Germany*
[b] *Unite de Pharmacie, Universite Catholique de Louvain, Brussels, Belgium*
[c] *Harvard-MIT Division of Health Science and Technology, Cambridge, MA, USA*

Received 6 July 1998; revised 22 August 1998; accepted 11 September 1998

Abstract

Application of 'high voltage' (HV) pulses (transdermal voltage $U_{skin} > 50$ V) to preparations of human skin have been previously hypothesized to cause electroporation of multilamellar lipid barriers within the stratum corneum (SC). Such pulses cause large increases in molecular transport and decrease in the skin's electrical resistance. Here we describe the local transport regions (LTRs) and the surrounding local dissipiation regions (LDRs) that dominate the skin's response to both 'long' and 'short' HV pulses. The number of LTR/LDRs depends on U_{skin}, but their size depends on pulse duration, so that LDRs can merge to form large regions containing several LTRs. LTRs themselves are not spatially homogeneous, as they have a ringlike structure, which is interpreted as involving different transport behavior viz. aqueous pathways which are either predominantly perpendicular or parallel to the SC. Our observations are consistent with the hypothesis that localized aqueous pathway formation (electroporation) occurs first, followed by secondary processes involving the entry of water into the SC and also localized heating.

Keywords: Human skin; Local transport regions; Local dissipation regions; Electroporation; Iontophoresis; Local heating

1. Background

The stratum corneum (SC) is the outermost, essentially dead layer of the skin. Even though thin (about 20 μm) [1], the SC is the primary barrier to entry of ions and molecules into the body [2–4]. This barrier therefore protects the underlying tissue and the body from infectious agents, toxic compounds, and water loss. Uncontrolled compromise of the skin's barrier function is therefore generally undesirable. However, for transdermal drug delivery the SC's barrier must be overcome. Understanding basic features of transdermal molecular and ionic transport is therefore important, and motivated the present study of the highly localized transport that results from the application of HV pulses.

The use of low voltages (< 5 V) to drive molecular transport across the skin by iontophoresis is well known [5,6], but neither the mechanism of transport at the molecular level nor the location of transport pathways is fully understood [7–10]. It is generally believed that preexisting aqueous pathways provide the main iontophoresis transport routes. More specifically, much of the transport is often associated with hair follicles and sweat ducts, where transport involves local electrophoresis. Moreover, it is believed that insignificant structural changes in the SC accompany iontophoresis, and that instead electrically driven entry of higher ionic strength electrolyte into preexisting aqueous pathways lowers the SC resistance and increases transport [11].

In contrast, HV pulses cause rapid, large increases in molecular and ionic transport [12–14]. As in single bilayer membrane barriers, these pulses are hypothesized to create new aqueous pathways, and to simultaneously provide a local electrical driving force, which together leads to a transport enhancement for charged species by orders of magnitude.

The onset of the response of the skin to 'high voltage' pulses is very rapid on the order of 10^{-6} s [15,16]. For a typical in vitro experiment with a skin specimen ($A_{skin} \approx 0.7$ cm^2), the external resistance between the electrodes and the skin is of order $R_{bulk} \approx 100\ \Omega$ and the skin

* Corresponding author. Tel.: +49-521-106-6261; e-mail: uwe.pliquett@post.uni-bielefeld.de

0302-4598/98/$ - see front matter
PII: S0302-4598(98)00180-9

capacitance (due mostly to the SC) is of order $C_{skin} \approx 10$ nF. Thus, the charging time constant is of order $R_{bulk} \cdot C_{skin} = \tau_{CHG} \approx 1$ μs. The observed time scale of aqueous pathway creation is similar [16]. In contrast, molecular transport across the skin cannot be readily measured for times shorter than a few seconds [17]. The largest change in R_{skin} occurs during the first pulse, consistent with the idea that new aqueous pathways are rapidly created, followed by some recovery. Subsequent pulses yield further but smaller resistance drops, which is consistent with the creation of still more pathways or enlarging of already created pathways. Moreover, an approximate plateau is observed for the dependence of molecular transport on U_{skin} for interpulse times shorter than 10 s [18]. Finally, the recovery of the skin after 'high voltage' pulsing is similar to artificial and cell bilayer membrane electroporation [18]. Here, the skin resistance, R_{skin}, recovers almost completely on a time scale ranging from less than seconds up to minutes for the smaller, shorter 'high voltage' pulses. There is a progression to negligible recovery for larger pulses. Significantly, electroporation is believed to be a non thermal phenomenon, in which rapid, electrostatically driven structural rearrangements take place before any significant heating occurs [19]. However, subsequent Joule heating may raise the temperature of the electrolyte within the aqueous pathways.

Localization of molecular and ionic transport across skin subjected to HV pulses has been only partially characterized in previous studies, which involved real time video recording of fluorescence microscopy, electrochemical deposition imaging based on the formation of light-absorbing AgCl by Cl^- ions, temporary confinement of transported molecules within a thin gel (agarose) layer held next to the skin on the receptor side ('gel localized microscopy' = GLM; [20]), and confocal microscopy [21].

These previous studies of local transport regions (LTRs) demonstrated that the current density is maximal in the center of a LTR but does not decay immediately at the borders of the LTR. By using GLM most of the molecules were found at center of the LTR's which implies that the sites involved in molecular transport occupy only a fraction of the entire region involved in transport (ionic and molecular) [20]. In comparison to a bilayer membrane thickness (about 4 nm), transport across the SC involves relatively long pathways (about 20 μm), i.e., a factor of $\approx 4 \times 10^3$ longer. Thus, although single bilayer membrane is believed to involve small local temperature increases due to the secondary process of ohmic dissipation, the amount of local heating can be significant for skin [15,22–25] but is behind the scope of this study.

2. Materials and methods

We used multiple parameter measurements for each skin preparation, which is important because of variability of biological specimens.

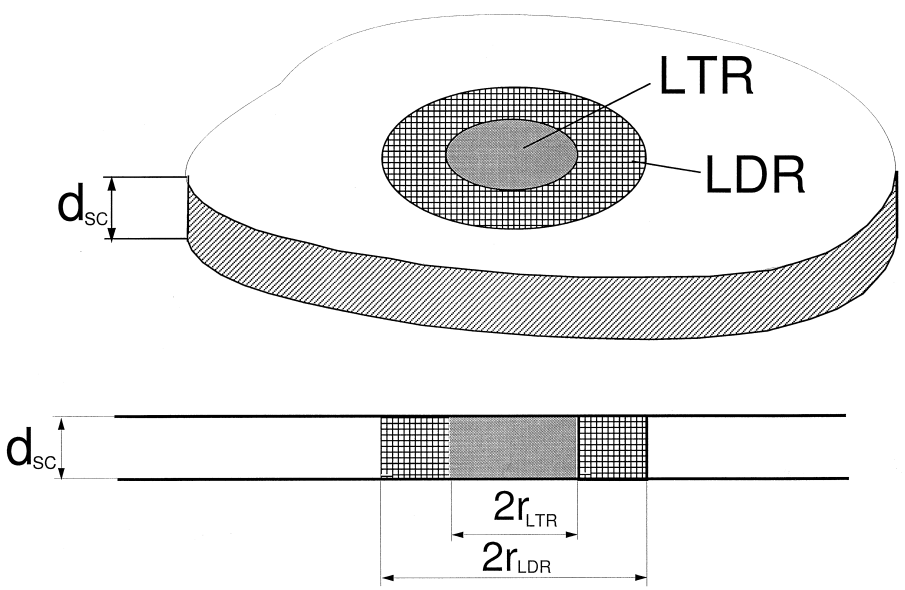

Fig. 1. Idealized drawing of the outer layers of the skin, showing the hypothetical structure of a local transport region (LTR) contained within a local dissipation region (LDR). Our results support the interpretation that small ion transport is concentrated within the LDRs, and that molecular transport is even more localized, occurring within the smaller LTRs. Here, a LTR is represented by a cylindrical region, with a thickness of the SC (d_{SC} = 10 to 20 μm) and a radius (r_{LTR} = 10 to 100 μm), which is strongly dependent on 'high voltage' pulse duration. The larger, concentric cylinder represents an idealized local dissipation region (LDR), whose sizes also depend on pulse length. All observations to date show that area of LDRs is larger than this of LTRs.

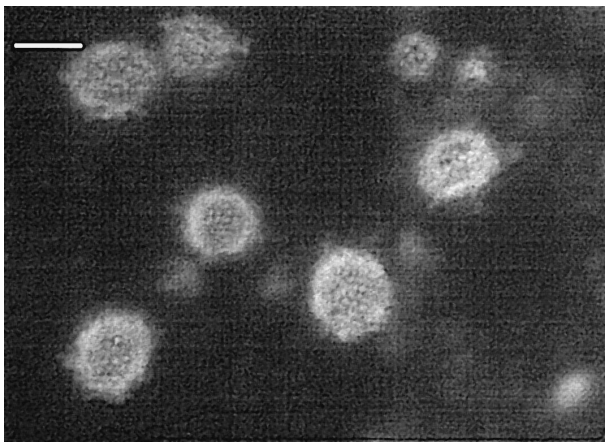

Fig. 2. Real time image of large LTRs involved in calcein (green fluorescence) transport due to medium HV pulses. Here, $U_{skin,0} \approx 30$ V for $\tau_{pulse} = 300$ ms, $N_{pulse} = 5$ and $T = 25 \pm 1$°C. The white bar has a length of 250 μm.

2.1. Skin preparation

We used heat stripped skin (thickness of about 50 μm, ≈ 20 μm stratum corneum and 30 μm of underlying epidermal tissue). The preparations were placed on waxed paper, stored refrigerated and used within two weeks.

2.2. 'High voltage' (HV) pulsing and transdermal voltage (U_{skin}) measurements

As described previously [15,16], a skin specimen was placed into a side-by-side permeation chamber equipped with outer pulsing electrodes and inner measurement electrodes. The pulsing anode was silver, the cathode stainless steel, and for measurement of U_{inner} Ag/AgCl electrodes were used. A number of pulses was applied, with interpulse spacing ranging from 5 s to 6 min (see figure captions). The current passing through the chamber was calculated from the voltage drop across a series 5 Ω resistor and stored in a digital oscilloscope together with the voltage across the inner electrodes. The transdermal voltage was then determined using $U_{skin}(t) = U_{inner} - I(t)R_{saline}$, which explicitly accounted for the voltage drop across the saline between the sensing ('inner') electrodes.

2.3. Pulsing solution and fluorescent molecules

The donor compartment of the chamber contained phosphate buffered saline (PBS; pH 7.4) and two water soluble fluorescent tracer molecules (calcein, Sigma; 623 g mol^{-1}, charge, $z = -4$; 1 mM) and (sulforhodamine, Sigma; 601 g mol^{-1}, $z = -1$; 1 mM).

2.4. Real-time imaging of fluorescent molecule transport sites

A small chamber was used with a fluorescence microscope for real-time visualization of transdermal transport [20]. This apparatus allowed the SC to be illuminated with fluorescence excitation light through the receptor compartment. To prevent illumination of the donor solution containing a high concentration of fluorescent molecules, a black filterpaper was placed at the epidermis side. Further reduction of excitation light was achieved by providing methylene blue in the donor compartment, which effectively absorbed excitation light. Both the receptor and the donor compartment had flow-through capabilities in order to remove liberated gas bubbles and fluorescent molecules which crossed the SC and to prevent a degradation of the donor solution by electrochemical byproducts. A video camera and VCR were used to acquire and store the images. For subsequent data analyses, some images were transferred to a computer (Macintosh, Apple Computer), and subsequently analyzed by MATLAB (The MathWorks, Natick, MA) software on a computer workstation (Sparc10, Sun Microsystems).

2.5. Post pulse imaging of molecular transport sites

After pulsing, the skin specimen was removed from the chamber and placed under a fluorescence microscope (Olympus BH2). By changing the illumination, it was possible to distinguish between sweat duct openings and hair follicles (incandescent illumination), and local transport regions (LTRs, blue excitation). As depicted schematically in Fig. 1, an LTR is a region wherein fluorescent molecule transport is concentrated, while a local dissipiation region (LDR) is a region where ionic transport only occurs. As reported in previous experiments using only 'short' pulses ($\tau_{pulse} \approx 1$ ms), some fluorescent molecules are retained long after pulsing ceases, even after washing, leading to characteristic ring-like images [21], which were identified as LTR.

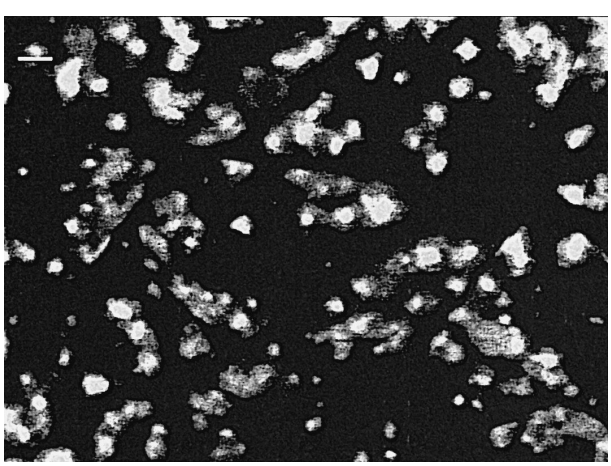

Fig. 3. Green image (calcein, real time) of small LTRs created by short HV pulses. Here, $U_{skin,0} \approx 60$ V in a sequence of $N_{pulse} = 5$ pulses at intervals of $t_{'int'} = 1$ min. These short exponential pulses had a time constant of $\tau_{pulse} = 1$ ms. The temperature was held at 25 ± 1°C. The LTR sizes are much smaller than in Fig. 2., with radii ranging from $r_{LTR} \approx 40$ to 100 μm. The scale bar is 100 μm.

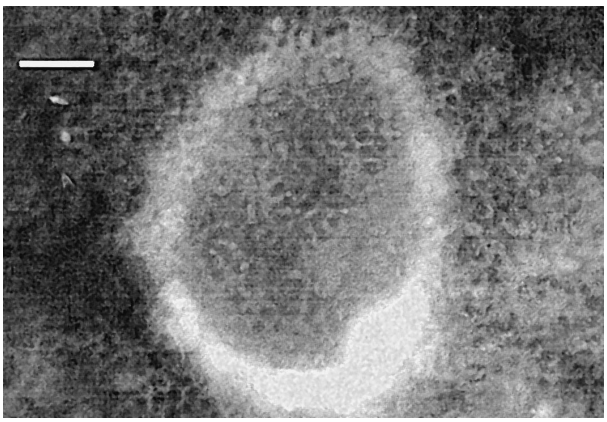

Fig. 4. Computer processed red fluorescence image (sulforhodamine) of a large (radius, $r_{LTR} \approx 250$ μm; scale bar, 250 μm) LTR created by 'medium high voltage' pulsing ($U_{skin,0} \approx 40$ V for $\tau_{pulse} = 200$ ms, $N_{pulse} = 20$ at 25 ± 1°C). In contrast to Fig. 3, these images were taken after the experiment, with the skin specimen mounted on a microscope slide. Many pericellular-red fluorescence-stained corneocytes are visible with a bright ring. Unlike the case of 'high-voltage' pulses, such LTRs have often an appendage at their centers, which we interpret as involvement of preexisting aqueous pathways. This is in marked contrast to the behavior found at high transdermal voltage ($U_{skin} > 60$ V). Here. the transdermal molecular transport across the skin is considerably greater than with large HV pulses.

GLM (gel localizing microscopy) prolongs localization of transported molecules upon their arrival at the receptor side, and was therefore used to demonstrate that these sites involve molecular transport across the SC [20]. Briefly, a thin (1 mm) agarose disk (2% agarose, medium melting point, Sigma) was placed next to the skin on the receptor side. This method was found to provide significant temporary localization of the transported fluorescent molecules. Use of this technique allowed demonstration that the gel-localized fluorescence was generally aligned with fluorescence of LTRs within the SC.

2.6. Electrochemical imaging of small ion transport

Small ions such as Na^+ or Cl^- are neither fluorescent nor light absorbing in a way that usefully contributes to a contrast mechanism for microscopy. Thus, an electrochemical method was used to visualize LDRs, within which electrical current due to small ion transport was concentrated [20]. A polished silver plate used as anode was placed behind the skin during pulsing. The reaction $Ag^+ + Cl^- \rightarrow AgCl$ takes place at the silver surface, where the almost insoluble and optically absorbing ('dark') AgCl forms deposits at the silver surface. This allowed identification of those regions with concentrated Cl^- transport, which, we assume also experienced comparable transport of Na^+. Thus regions with large AgCl deposits are interpreted as corresponding to regions with the high electrical current density.

2.7. Laser scanning confocal microscopy

To obtain information about the depth of the retaining fluorescent molecules within the SC, skin specimens were placed under a laser scanning confocal microscope (Bio-Rad on Zeiss-stative). Calcein and sulforhodamine were visualized simultaneously (filter block K2).

3. Results

3.1. General observations

We distinguish two voltage and two pulse duration regions, in which U_{skin} is used rather than the voltage applied to the electrodes U_{elec}. $U_{skin} \approx U_{SC}$ due to the much greater electrical conductivity of the dermis. A variable voltage divider effect between the electrode–electrolyte system and the skin results in reduced electrode voltage appearing across the skin [16]. Here, for example, application of 750 to 1500 V across the chamber's electrodes results in a peak 'large high voltage' of only $U_{skin,0} \approx 100$ V. Similarly, a pulse with a peak value of 50 to 400 V at the electrodes gives a 'medium high voltage' pulse at the skin $U_{skin,0} \approx 20$ to 60 V. Pulses were also distinguished by their duration, viz. their time constants, τ_{pulse}. Pulses with $\tau_{pulse} > 5$ ms (usually > 100 ms) are referred as 'long pulses' pulses while pulses with $\tau_{pulse} < 5$ ms (usually 1 to 2 ms) are referred to as 'short pulses'.

3.2. Number and size of local transport regions (LTRs)

Previous investigations using only 'short pulses' found that LTRs had diameters less than about 100 μm [20,21]. Here we also used much longer exponential pulses ($\tau_{pulse} = 100$ to 400 ms), for which the size of LTRs was larger,

Fig. 5. Fluorescence images of small LTRs created by HV pulsing. Here, $U_{skin,0} \approx 60$ V for most of the pulses in a sequence of $N_{pulse} = 30$ pulses at intervals of $t_{'int'} = 1$ min. As in Fig. 4, the specimen was washed for one day before taking the pictures. These short exponential pulses had a time constant of $\tau_{pulse} = 1$ ms at 25 ± 1°C. The LTR sizes are much smaller than in the preceding figures, with radii ranging from $r_{LTR} \approx 40$ to 100 μm. The large number of LTRs resulted in many LTRs being created near previously existing LTRs, and the associated larger LDRs had considerable overlap. The scale bar is 100 μm.

with diameters up to $2r_{LTR} \approx 600$ μm. Further, as also found in previous work for short pulses, the pulse voltage U_{elec} is less important for LTR size than for LTR number. Specifically, if $U_{skin,0}$ is increased the number of LTR increases, while their shape and size depends on pulse duration. Figs. 2 and 3 show real time images for two extreme cases: long lasting medium voltage pulses, and short high voltage pulses.

3.3. Morphology and time-dependence of the LTR-fluorescence

LTRs are characterized by significantly different regions, which are distinguished by the two charged fluorescent molecules, calcein and sulforhodamine. If an LTR is created by short, large HV pulses, different regions can be seen shortly (typically less than 10 min) after pulsing as

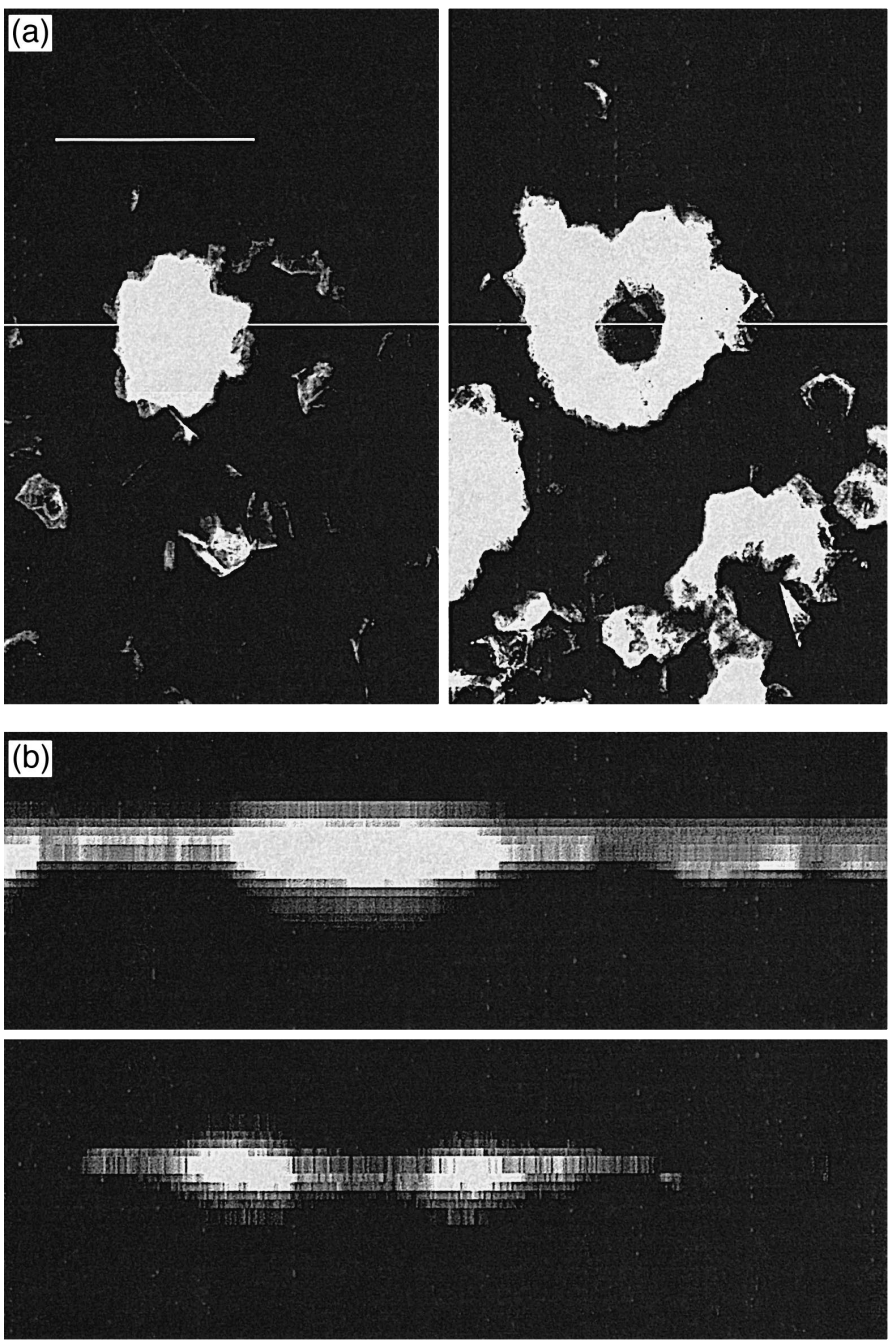

Fig. 6. Confocal image with 10-μm depth into the SC. The skin was pulsed 60 times with $U_{skin} \approx U_{SC} \approx 105$ V, and after pulsing washed for 1 h. The left side (scale bar, 200 μm) is the red fluorescence image (sulphorhodamine). The green (calcein) image is shown right. (B) (two parts) Cross-section of the same specimen along the white line in (A). The top portion is based on the red fluorescence of sulforhodamine, showing some generalized distribution at low levels, but a concentrated distribution within the LTR. Conversely, the bottom portion is based on the green fluorescence of calcein, showing the distribution along the rim (edge) of the LTR.

having a 'fine structure' that corresponds to the corneocytes, which are internally stained by both fluorescent molecules [20]. However, if the skin is removed from the chamber and then immersed in PBS without the fluorescent molecules present, within 2 to 10 h, the central intensely fluorescent region of the LTR becomes dark, with only a bright fluorescent ring remaining (Figs. 4 and 5).

The distribution of the remaining dye within the ring structure can be seen by confocal microscopy (Fig. 6) where different behavior in spreading between the calcein and sulforhodamine are found. Comparison of the cross-sectional fluorescence intensity distribution shows that the ring structure of calcein is much more pronounced at this time (1 h after pulsing) than of sulforhodamine (Fig. 7).

Application of 'long pulses' using 'medium high voltages' results in even more pronounced ring-like structures for LTRs and LDRs. However, within the center region of LTRs, the outlines of corneocytes are often still visible (Fig. 4). A bright ring marking the periphery of the LTR is visible immediately after the pulsing, in contrast to the use of 'large high voltage' pulses.

3.4. Local dissipation regions (LDRs)

Examination of the AgCl images on the underlying planar silver anode provided visualization of the resistivity distribution over the SC, with a ring-like structure also evident. Although a central low resistivity region with a sharp edge was found, LTRs are surrounded by a diffuse ring of low resistivity (LDR) which is larger than the central low resistivity region of the LTR (Figs. 8 and 9).

Although LDRs are larger than LTRs, they nevertheless occupy only a fraction of the entire skin area. Even the transport of the charged fluorescent molecules occurs mainly at the center of a LTR which was evident from experiments with GLM.

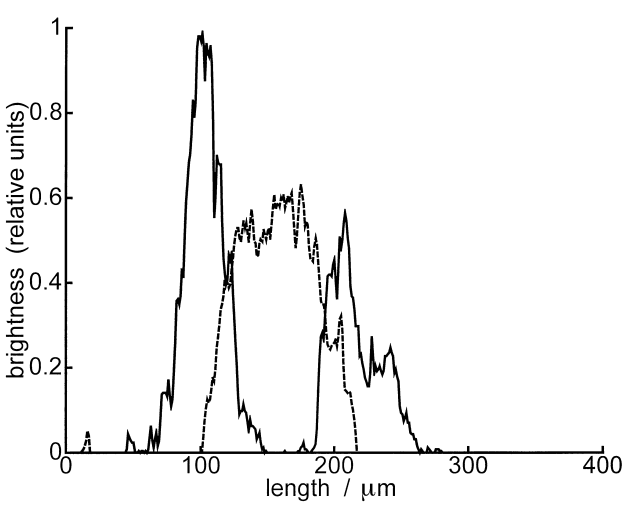

Fig. 7. Cross-sectional histogram for the image in Fig. 6 along the white line (solid line—calcein, dashed line—sulforhodamine).

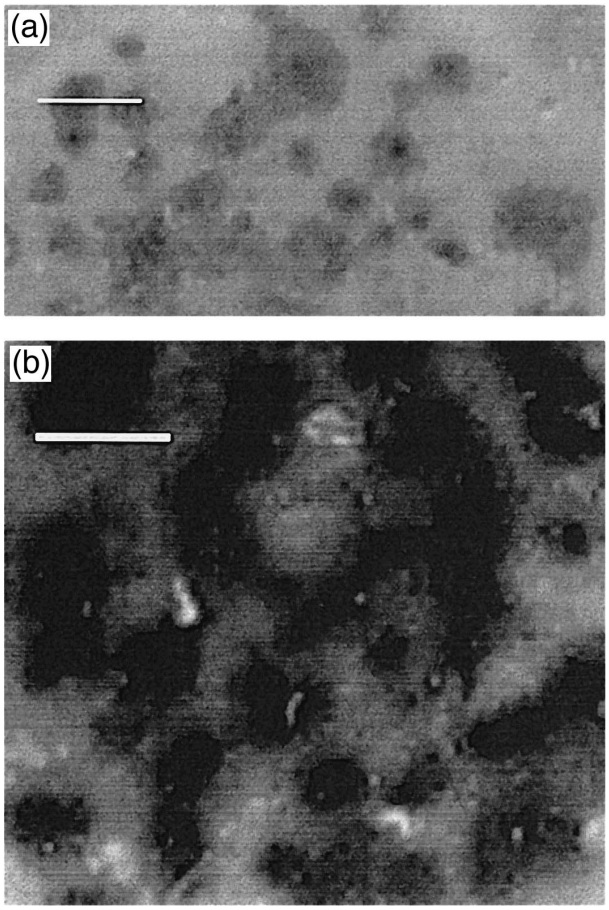

Fig. 8. Electrochemical images based on AgCl deposits on a Ag anode located behind a skin specimen. (A) $N_{pulse} = 60$ large HV pulses with $\tau_{pulse} = 1$ ms using $U_{electrode} = 1000$ V, which resulted in $U_{skin,0} \approx 100$ V. (B) $N_{pulse} = 20$ medium HV pulses with $\tau_{pulse} =$ ms using $U_{electrode} = 400$ V, which resulted in $U_{skin,0} \approx 40$ V.

3.5. LDR vs. LTR

Because LDRs are sometimes much larger than LTRs, LDRs merge, forming large, high conductive regions.

3.6. Temperature changes due to local heating within an LTR and LDR

In the absence of bulk electrochemical reactions, the passage of electrical current through a resistive medium causes only heating. Because the effective fractional aqueous area involved in ionic transport, $F_{w,ions}$ during pulsing is relatively small ($F_{w,ions} \approx 0.1$) [18], and the current passing through the skin is in the order of 2 A/cm^2 at a transdermal voltage up to 120 V, significant local heating may occur. This problem has been considered in detail using several types of temperature measurements [24] and also by carrying out idealized theoretical calculations for heat transfer in LTR/LDRs [25]. The essential results of these studies are summarized here, to assist the interpretation of the present imaging results. Briefly, the spatially

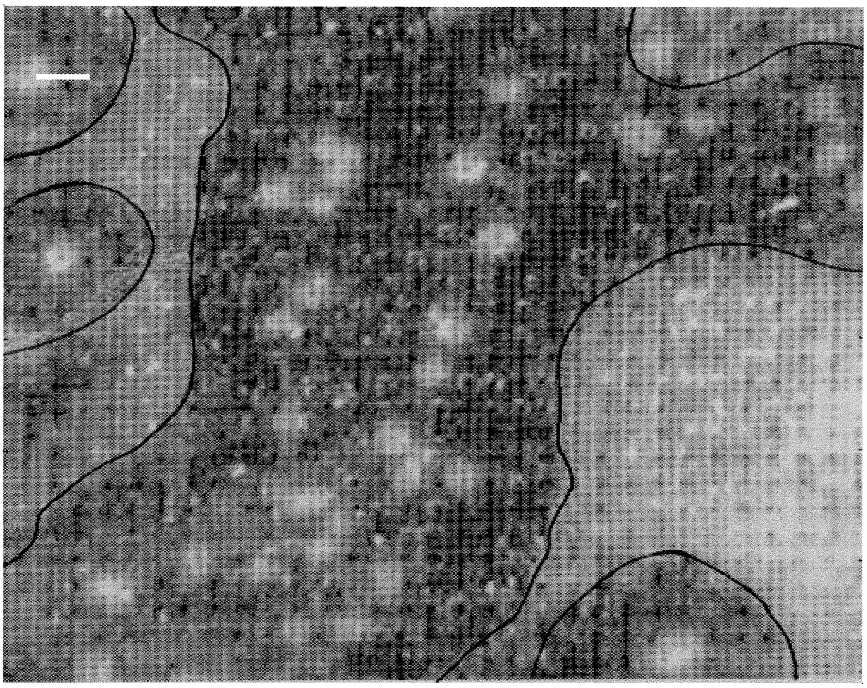

Fig. 9. Combined image based on two color fluorescence (calcein and sulforhodamine), and on light absorption by AgCl deposits after 30 pulses (anode—silverplate, $U_{skin} \approx 60$ V, $t_{pulse} \approx 1$ ms). The green fluorescent and red fluorescent spots within large dark regions indicate LTRs for charged fluorescent melecule transport within merged LDRs for electric current due to small ions. The larger bright areas are glare from the high reflectively Ag surface that have insignificant AgCl deposits (boundaries marked with pencil). The electrochemical image based on dark AgCl deposits indicates the spatial distribution of time integrated Cl^- ion transport.

averaged temperature change over the LDR did not exceed 20 K for pulses with $U_{skin} = 80$ V and $\tau_{pulse} = 1$ ms ('short pulse' and 'large high voltage'). However, for 'long pulses' with $\tau_{pulse} > 100$ ms, the temperature rise was larger, so that 70°C was exceed within the LDRs. The overall conclusion of these other studies is that (1) only small, generally negligible average (!) heating occurs for 'short pulses', even using 'large high voltage' pulses, but (2) 'long pulses' lead to significant temperature rise, even for 'medium high voltage' pulses.

4. Discussion

Both 'short' and 'long pulses' with 'medium' and 'large high voltages' are associated with localized ionic and molecular transport, i.e., LDRs and LTRs are involved. However, the mechanism of enhanced transport and the type of overall structural changes appears to be different for the 'short' and 'long pulses'. As an aid to understanding the detailed discussion of our results, an overview of our observations and their interpretation is presented first. Our results are consistent with the hypothesis that short, large HV pulses are associated with a primary event of spatially localized electroporation of bilayer membranes within the stratum corneum.

4.1. Short high-voltage pulses ($\tau_{pulse} < 5$ ms, $U_{skin} > 50$ V)

Pulses of 750 to 1500 V (high voltage range) across the electrodes resulted in much smaller peak transdermal voltages, $U_{skin,0} \approx 100$ V (± 30 V). The response of the SC to the increased U_{skin} involves both LDRs and LTRs. Reversible as well as irreversible structural changes were found. Significant recovery of the transdermal barrier can occur, besides persistent structural changes. LTRs are revealed by fluorescence microscopy, but are usually not visible by ordinary light microscopy. Secondary events are believed to include: (1) entry of water into much of the SC, which contributes to both, lateral molecular transport and visualization of fluorescent molecules within the SC, and (2) localized heating within LDRs, with the largest temperature changes within the LTRs.

4.2. Long medium-voltage pulses ($\tau_{pulse} > 100$ ms, $U_{skin} < 60$ V)

In contrast, 'long pulses' appear to involve considerable heating by electrical dissipation in aqueous pathways subsequent to electroporation, i.e., as a secondary process. The effect of the somewhat smaller U_{skin} was overwhelmed by the approximately two orders of magnitude τ_{pulse}, and therefore significant local heating occurred. It is striking that with lower voltages the percentage of LTRs associated with a sweat duct increases tremendously while

at high voltages LTRs are never fall together with appendages. Thus, for the smaller 'medium high voltage' pulses, most of the changes are due to thermal effects associated with preexisting aqueous pathways (sweat ducts) where only a small number of lipid layers (≈ 4 in two cell layers) needs to be electroporated. Further support for the importance of heating comes from the comparison of the skin conductivity after long pulses with unpulsed skin exposed to elevated temperature above 70°C. Taken only the involved area (LDR) into account, in both cases a specific area conductivity of about 5 mS/cm^2 was found. This is consistent with a known phase transition of SC lipids from quasi crystal to liquid crystal state for temperatures between 65 and 75°C [26–28].

4.3. Time course of pathway creation within the stratum corneum

Electroporation of a multilamellar structure such as the stratum corneum is expected to be a complex phenomenon, with some aspects similar to electroporation of single bilayer membranes (artificial planar bilayer membranes and cell membranes) [29–31]. First, the voltage applied to the electrodes results in charging of the lipid barriers, such that the largest voltages appear across the barriers with the greatest resistance (here the approximately 100 bilayers of the multilamellar SC). There is strong evidence that electroporation of single bilayer membranes is fundamentally stochastic [30,31], so there is no actual critical voltage, but instead only an approximate threshold that depends on pulse duration. For individual bilayer membranes exposed to 'short pulses', a transmembrane voltage of $U \approx 0.5$ to 1 V is needed to create so many aqueous pathways ('pores') that the resulting high membrane conductance causes the transmembrane voltage to drop (often termed 'breakdown'). This first (primary) stage in which aqueous pathways are created is believed to be limited by barrier charging times of order $\tau_{CHG} \approx 10$ μs for single artificial or cellular bilayer membranes. Similar values govern charging of the SC [32]. Thus, for both 'short pulses' and 'long pulses' used here, the primary, onset phase is mainly controlled by SC charging, and the observed onset at $U_{skin} \approx 50$ to 100 V is consistent with electroporation hypothesis.

The second, main electroporation phase involves electrically driven transport of small ions and molecules through the then-existing aqueous pathways. In the case of single planar bilayer membranes, the transmembrane voltage is predicted to decay only slowly, even if the externally applied voltage pulse decays exponentially [33], and this provides a nearly constant electrical driving force for electrophoretic or electro-osmotic transport. The situation within the SC is more complex, but some features of single bilayer membrane electroporation are again evident. During the second phase the peak transdermal voltage is in the range $U_{skin,0} \approx 20$ to 120 V, and depends on the pulse magnitude. In our interpretation, variable voltage division is important, involving two parts of the system: (1) the electrodes and electrolyte (here PBS) external to the SC, and (2) the voltage across the SC, which to a good approximation is U_{skin}. For the chamber and electrodes used here, if $U_{electrode} < 1500$ V, then U_{skin} does not exceed about 120 V, and for 'short pulses' electrically driven transport occurs mainly during the pulses.

For 'short pulse' conditions the local heating within an LTR results in a spatially averaged temperature rise of less than 20 K from an initial value of 25 ± 1°C, so that the resulting temperature is 45°C, which does not imply that the phase transition temperature is not reached locally. This could explain the persistent changes found in R_{skin} within the LTR even for short pulses. During 'long pulses', the power dissipated within an LDR/LTR often results in a temperature rise to 70°C, so a phase transition for the sphingo-lipid membranes within the SC is triggered [26,27]. If this occurs during the pulse, secondary thermal effects are dominant allowing even more changes because of local electrical forces. Further, localized heating implies that lateral heat transport over relatively long times should be considered. Thus, the recovery phase of skin electroporation not only involves recovery of a multilamellar system perforated by aqueous pathways, but also slow recovery from thermally induced changes. Taken together, the results of this study lead to an interpretation of LDR/LTRs that may involve electroporation as a rapid primary event followed by slight heating for 'short pulses' and 'large high voltages', and significant localized heating for 'long pulses' at 'medium high voltages'. Further studies will be needed to clarify the detected nature of this response.

4.4. Kinetics of ionic and molecular transport

After charging of the SC's multilamellar barrier on a time scale of 10 μs, for large pulses electroporation occurs in inter-corneocyte bilayer membranes. One result is localized electropermeabilization, such that LDRs and LTRs are formed. During the pulse, a local electric driving force for ions and charged molecules is present and significant transport occurs through the then-existing aqueous pathways. This should be the case if the aqueous pathways are large enough to accommodate the fluorescent molecule. In addition to this primary effect of electroporation, there are important secondary phenomena. Our interpretation is that the ordinarily water-poor regions between the multilamellar bilayer membranes experience a large influx of water, with much of it becoming trapped once some aqueous pathway recovery begins. At the same time, the SC begins to heat, but with the largest temperature rise in the centers of LTRs, where the trans-stratum corneum resistivity is smallest. As evident from time resolved temperature imaging studies [24] a heat front propagates during the pulse, emerging form the center of an LTR. The edge of the LTR seems consistent with the region of a heat

front, where approximately 70°C was reached. This is supported by the fact that essentially permanent alteration of skin due to heating occurs if about 70°C was reached and the resistance of the interior of an LTR was found to be irreversible on the time scale of hours. Moreover, the area resistance of skin which was subjected to temperatures more than 70°C is about the same as in the center region of an LTR ($\approx 200\ \Omega\ cm^2$). It is unlikely that the expansion of the LTR is due to electric interactions, since the electric field within the surrounding region of an LTR is not increasing but decreasing, which prevents further electroporation of membranes. We suggest that the propagating heat front is associated with driving water laterally within the SC by pressure gradient arising from volume increase of the heated water. At the end of the pulse, the LDR/LTR cools, leaving behind a structurally altered region.

The transport properties of the LDR/LTR are anisotropic. The center of the LTR contains aqueous pathways which are effectively perpendicular to the SC, because they support transport across the SC. In addition, the immediate vicinity of the LTR now contains significant water, and supports lateral spreading of the water soluble calcein and sulforhodamine by diffusion. However, the edge of the LTR, the boundary between perpendicular and lateral pathways, has a lateral barrier function. We conclude this from the fact that even after hours of soaking in fresh saline sharp boundaries of LTR are visible, i.e., the center appears dark, while a bright fluorescent ring persists. If there were no barriers, the ring would be rather diffuse or would disappear. According to our interpretation, the edge of the LTR therefore involves a boundary that corresponds to the furthest propagation of the temperature rise needed to cause a order/disorder phase transition, indicated by the irreversible drop in R_{skin}. In the center of the LTR, local electrical forces, and possibly also local pressure gradients, have created the mostly perpendicular pathways. At the LTR boundary, however, the trans-stratum corneum pathways mostly recover, and this process effectively seals off the LTR interior. Calcein and sulforhodamine introduced into this region during the pulse become trapped, leaving the characteristic fluorescent ring. The trans-stratum corneum permeability of the LTR center does not recover. Without a driving force there is insignificant transport.

4.5. New structures for ionic and molecular transport

Imaging of LTRs in real time yields a uniformly stained center and no bright fluorescence borders of corneocytes for short pulses using large HV. This is consistent with the hypotheses that the entire corneocytes are involved in transport for large HV pulses, by creating straight through aqueous pathways that penetrate corneocytes. In contrast, long pulses at medium HV result in bright fluorescence staining around the edges of corneocytes, which suggests molecular transport around the corneocytes. LTR size (radius) is a function of the electrical power dissipated during the pulse. Thus, the boundary ('ring') of the LTR occurs at the site of the furthest extent of the temperature rise that reaches ≈ 70°C. Taking into account that the voltage across the skin differs only by a factor of five in going from medium HV to large HV, but the pulse duration varies by two orders of magnitude in going from short pulses to long pulses, LTR size is mostly determined by pulse duration, here characterized by τ_{pulse}. Earlier studies [20,21] used $\tau_{pulse} \approx 1$ ms, but different U_{skin}, and these pulsing protocols yielded a narrow distribution of LTR sizes.

4.6. Irreversible changes within the stratum corneum

Irreversible alteration may occur, i.e., the resistance of the SC is permanently lowered. The specific resistance of the SC inside the LTR after pulsing is about 200 $\Omega\ cm^2$ which is in good agreement with the behavior of skin heated to more than 70°C (without pulsing). Passive transport after pulsing is consistent with diffusion through the persistent high permeability regions (LTR).

5. Conclusion

The application of HV pulses to human stratum corneum may cause multilamellar electroporation within microseconds, followed by localized heating within small regions, involving up to 10% of the SC-surface. While the pulse lasts, the local electrophoretic driving force together with the newly created aqueous pathways yield a large transport of charged water soluble molecules. Joule heating occurs within the aqueous pathways and large thermal effects are responsible for expansion of permeable regions (LTR/LDR). The localized changes due to thermal effects are irreversible. LTR size is a function of pulse duration (τ_{pulse}), while LTR number increases with U_{skin}. This supports the hypothesis that the condition for electroporation are reached at larger fraction of the skin for higher voltage, and that heating during the pulse, resulting in a propagating heat front, expands the permeable region. At low pulsing voltage, mostly appendages (sweat ducts) are electroporated.

6. Important terminology, abbreviations and notation

'Long pulse'	Exponential pulse with $\tau_{pulse} \geq 5$ ms, usually ≈ 100 ms
'Short pulse'	Exponential pulse with $\tau_{pulse} \leq 5$ ms, usually ≈ 1 ms

'Medium high voltage'	Exponential pulse amplitude resulting in $U_{skin,0} = 30$ to 60 V and (50 to 400 V across electrodes in present chamber)
'Large high voltage'	Exponential pulse amplitude resulting in $U_{skin,0} > 60$ V and (750 to 1500 V across electrodes in present chamber)
LTR	Local transport region (here for calcein and sulforhodamine)
LDR	Local dissipation region (small ion transport, Cl^-, Na^+)
N_{pulse}	Number of identical pulses applied to electrodes
SC	Stratum corneum of skin (thickness, $d_{SC} \approx 10$ to 15 μm)
$U_{skin,0}$	Peak value of transdermal voltage
$U_{SC,0}$	Peak value of voltage across SC (approximately $U_{skin,0}$)
τ_{pulse}	Time constant of exponential pulse

Acknowledgements

We thank C.A. Gusbeth, T.E. Vaughan, E.A. Gift and Y. Chizmadzhev for many stimulating discussions and helpful criticisms. Supported by NIH grant ARH4921 and Whitaker Foundation grant RR10963.

References

[1] P.M. Elias, E.R. Cooper, A. Korc, B.E. Brown, Percutaneous transport in relation to stratum corneum structure and lipid composition, J. Invest. Derm. (1981) 297–301.
[2] L.A. Goldsmith, Physiology, Biochemistry, and Molecular Biology of the Skin, Oxford Univ. Press, New York, 1991.
[3] P.M. Elias, G.K. Menon, Structural and lipid biochemical correlates of the epidermal permeability barrier, J. Adv. Lip. Res. (1991) 1–26.
[4] E.W. Smith, H.I. Maibach, Percutaneous Penetration Enhancers, CRC Press, Boca Raton, FL, 1995.
[5] B.H. Sage, in: E.W. Smith, H.I. Maibach (Eds.), Percutaneous Penetration Enhancers, Iontophoresis, CRC Press, 1995, pp. 351–368.
[6] R.R. Burnette, Transdermal drug delivery, in: J. Hadgraft, R.H. Guy (Eds.), Developmental Issues and Research Initiatives, Iontophoresis, Marcel Dekker, New York, 1989, pp. 247–291.
[7] C. Cullander, R.H. Guy, Transdermal delivery of peptides and proteins, Adv. Drug Deliv. Rev. (1992) 291–329.
[8] N.A. Monteiro Riviere, A.O. Inman, J.E. Riviere, Identification of the pathway of iontophoretic drug delivery: light and ultrastructural studies using mercuric chloride in pigs, Pharm. Res. 11 (1994) 251–256.
[9] E.R. Scott, H.S. White, J.B. Phipps, Iontophoretic transport through porous membranes using scanning electrochemical microscopy: application to in vitro studies of ion fluxes through skin, Anal. Chem. 65 (1993) 1537–1545.
[10] J.C. Weaver, Y.A. Chizmadzhev, in: C. Polk, E. Postow (Eds.), CRC Handbook of Biological Effects of Electromagnetic Fields, Electroporation, CRC Press, Boca Raton, FL, 1996, pp. 247–274.
[11] S.M. Dinh, C.W. Luo, B. Berner, Upper and lower limits of human skin electrical resistance in iontophoresis, AIChE J. (1993) 2011–1018.
[12] U. Pliquett, J.C. Weaver, Transport of a charged molecule across the human epidermis due to electroporation, J. Controlled Release (1996) 1–10.
[13] R. Vanbever, E. LeBoulenge, V. Preat, Transdermal delivery of fentanyl by electroporation: I. Influence of electrical factors, Pharm. Res. 13 (1996) 559–565.
[14] T.E. Zewert, U. Pliquett, R. Langer, J.C. Weaver, Transdermal transport of DNA antisense oligonucleotides by electroporation, Biochem. Biophys. Res. Commun. 212 (1995) 286–292.
[15] U. Pliquett, J.C. Weaver, Passive electrical properties of human stratum corneum during application of electric fields, in: F. Bersani (Ed.), Electricity and Magnetism in Medicine and Biology, 1998.
[16] U. Pliquett, R. Langer, J.C. Weaver, Changes in the passive electrical properties of human stratum corneum due to electroporation, BBA 1239 (1995) 111–121.
[17] U. Pliquett, M.R. Prausnitz, Y.A. Chizmadzhev, J.C. Weaver, Measurement of rapid release kinetics for drug delivery, Pharm. Res. 12 (1995) 549–555.
[18] U. Pliquett, J.C. Weaver, Electroporation of human skin: simultaneous measurement of changes in the transport of two fluorescent molecules and in the passive electrical properties, Bioelectrochem. Bioenerg. (1996) 1–12.
[19] E. Neumann, A. Sowers, C. Jordan, Electroporation and Electrofusion in Cell Biology, Plenum, New York, 1989.
[20] U. Pliquett, T.E. Zewert, T. Chen, R. Langer, J.C. Weaver, Imaging of fluorescent molecule and small ion transport through human stratum corneum during high-voltage pulsing: localized transport regions are involved, Biophys. Chem. 58 (1996) 185–204.
[21] M.R. Prausnitz, J.A. Gimm, R.H. Guy, R. Langer, J.C. Weaver, C. Cullander, Imaging regions of transport across human stratum corneum during high voltage and low voltage exposures, J. Pharm. Sci. (1996) 1363–1370.
[22] U. Pliquett, C. Gusbeth, F. Pliquett, in: J.R. Riu, J. Rosell, R. Bragos, O. Casas (Eds.), Proceeding of the X. International Conference on Electrical Bio-Impedance, Barcelona, Spain, Perturbation of human stratum corneum: electric field application vs. heating, Publications Office of UPC, Barcelona, 1998, pp. 277–280.
[23] U. Pliquett, Mechanism of skin electroporation, Adv. Drug Deliv. Rev. (1998) in press.
[24] U. Pliquett, G.T. Martin, J.C. Weaver, Kinetics of temperature rise within the stratum corneum during electroporation and pulsed high voltage iontophoresis, 1998, submitted.
[25] G.T. Martin, U. Pliquett, J.C. Weaver, Temperature rising during tissue electroporation: theoretical modeling, 1998, submitted.
[26] R.M. Hatfield, L.W. Fung, Molecular properties of a stratum corneum model lipid system: large unilamellar vesicles, Biophys. J. 68 (1995) 196–207.
[27] S. Kitagawa, N. Yokochi, N. Murooka, PH-dependence of phase transition of the lipid bilayer of liposomes of stratum corneum lipids, International Journal of Pharmaceutics (1995) 49–56.
[28] T. Ogiso, H. Ogiso, T. Paku, M. Iwaki, Phase transitions of rat stratum corneum lipids by an electron paramagnetic resonance study and relationship of phase states to drug penetration, BBA (1996) 97–104.
[29] D.C. Chang, B.M. Chassy, J.A. Saunders, A.E. Sowers, Guide to Electroporation and Electrofusion, Academic Press, New York, 1992.
[30] J.C. Weaver, Y.A. Chizmadzhev, in: C. Polk, E. Postow (Eds.),

CRC Handbook of Biological Effects of Electromagnetic Fields, Theory of Electroporation: a Review, CRC Press, Boca Raton, FL, 1996, pp. 247–274.
[31] J.C. Weaver, Electroporation: a general phenomenon for manipulating cells and tissue, J. Cellular Biochem (1993) 426–435.
[32] S. Kakorin, E. Neumann, Chemical electrooptics and linear dichroism of polyelectrolytes and colloids, Ber. Bunsenges. Phys. Chem. 100 (1996) 721–722.
[33] S.A. Freeman, M.A. Wang, J.C. Weaver, Theory of electroporation for a planar bilayer membrane: predictions of the fractional aqueous area, change in capacitance and pore–pore separation, Biophys. J. (1994) 42–56.